JOURNAL OF SPACECRAFT AND ROCKETS
Vol. 32, No. 3, May–June 1995

Nonlinear Forced-Response Characteristics of Contained Fluids in Microgravity

M. C. van Schoor*
University of Pretoria, Pretoria, South Africa
and
E. F. Crawley†
Massachusetts Institute of Technology, Cambridge, Massachusetts 02139

An experimental study of the change in the lateral slosh behavior of contained fluids between earth and space is presented. The experimental apparatus used to determine the slosh characteristics is described, and a nonlinear analytical model of a coupled fluid-spacecraft system is outlined. The forced-response characteristics of silicone oil distilled water in a cylindrical tank with either a flat or a spherical bottom are reported and discussed. A comparison of the measured earth and space results identifies and highlights the effects of gravity on the linear and nonlinear slosh behavior of these fluids.

Nomenclature

a = tank radius, cm
Bo = bond number
D = damping constant
d = tank diameter, cm
f = equilibrium free-surface shape function
F_{ex} = forcing amplitude, N
g = apparent gravity level, m-s^{-2}
h = average fluid depth, cm
K_{Fx} = planar slosh force sensitivity, V/N
K_{Fy} = nonplanar slosh force sensitivity, V/N
K_x = displacement sensitivity, V/mm
K_{ax} = acceleration sensitivity, V/m-s^{-2}
m_f = fluid mass, kg
q_1 = first fluid slosh degree of freedom, cm
r = radial coordinate, cm
U_σ = capillary potential energy, J
x = tank planar displacement, cm
x_{ex} = tank excitation displacement, cm
y = tank nonplanar displacement, cm
z = displacement along tank symmetry axis, cm
α = fluid–tank-well contact angle deg, rad
ζ_{q_1}, ζ = damping ratio
η = free-surface shape function
λ = mass fraction of fluid participating in resonant motion
ν_K = kinematic viscosity cm^2/sec
μ = fluid-to-spacecraft mass ratio
ν = first-slosh-to-spacecraft frequency ratio
ρ = fluid density kg m^{-3}
σ = surface tension dyne/cm
ϕ = fluid flow potential function
ω_s = natural frequency of first slosh mode, Hz

Introduction

THE precise operating requirements of modern spacecraft demand a detailed model of all of the dynamic components of the system, including the dynamics of onboard contained fluids. This modeling requirement becomes more important as spacecraft increasingly rely on higher-efficiency liquid propellants. Since the nonlinear fluid-spacecraft motion caused by finite-amplitude fluid slosh departs significantly from the motion predicted by linear theory, the standard approach of using linearized models of the contained-fluid dynamics for structural and control analyses is inadequate for addressing this problem.[1]

The theory of nonlinear fluid slosh, despite the contributions of many researchers and experimenters, is still one of the areas of classical fluid dynamics that is not well understood. Contained fluids onboard spacecraft exhibit nonlinear dynamic characteristics that were, in the past, routinely avoided by conservative spacecraft designs. These characteristics, if unmodeled, can adversely affect the performance and stability of the spacecraft and lead spacecraft designers to conservative designs, with associated mass and cost penalties.

The importance of the slosh characteristics of contained fluids is reflected by the research efforts of the engineering and science communities,[2–6] in particular in the former Soviet Union.[7–10] Since 1985, researchers at Massachusetts Institute of Technology (MIT) have developed a nonlinear, nonplanar contained-fluid–spacecraft model. This model was verified for one-gravity conditions by comparing predicted slosh forces with those measured for an extensive test matrix on fluids contained in cylindrical, spherical, and rectangular tanks.[1] However, given that gravity has a significant influence on the modal characteristics of contained fluids, a shuttle experiment was proposed to the NASA INSTEP program. In 1988, OAST funded this proposal as the Middeck 0-gravity Dynamics Experiment (MODE). The prime objectives of the MODE fluid slosh experiments were: to provide a fundamental insight into the lateral oscillatory behavior of contained fluids in microgravity, typical of those found in on-orbit fluid tanks; to provide data for calibrating and verifying a well-posed model of such phenomena; and in doing so to provide the basic scientific and practical engineering knowledge needed to design space-based systems such as fuel depots and other fluid storage systems.

MODE flew on board STS-48 in September 1991, and was operated by astronauts Col. Jim Buchli and Col. Mark Brown. Although MODE also investigated the effects of gravity on the modal characteristics of jointed truss structures,[11] this paper focuses on its ground and space experimental results on fluids. The purpose of the paper is not only to present the MODE results but also to examine and highlight differences between the space and ground fluid slosh dynamics.

The first part of the paper describes the MODE hardware and fluid test articles. As a motivation for investigating nonlinear slosh, the hardware description is followed by a summary of the major sources of nonlinearity in the slosh dynamics and their variation with apparent gravity. The paper then presents the ground and space experimental results, and concludes with a discussion of the trends in these results.

Received Feb. 6, 1993; revision received May 16, 1994; accepted for pulication May 19, 1994.

*Professor of Mechanical Engineering and Visiting Principal Research Scientist, Massachusetts Institute of Technology. Member AIAA.

†Professor of Aeronautics and Astronautics and MacVicar Faculty Fellow. Fellow AIAA.

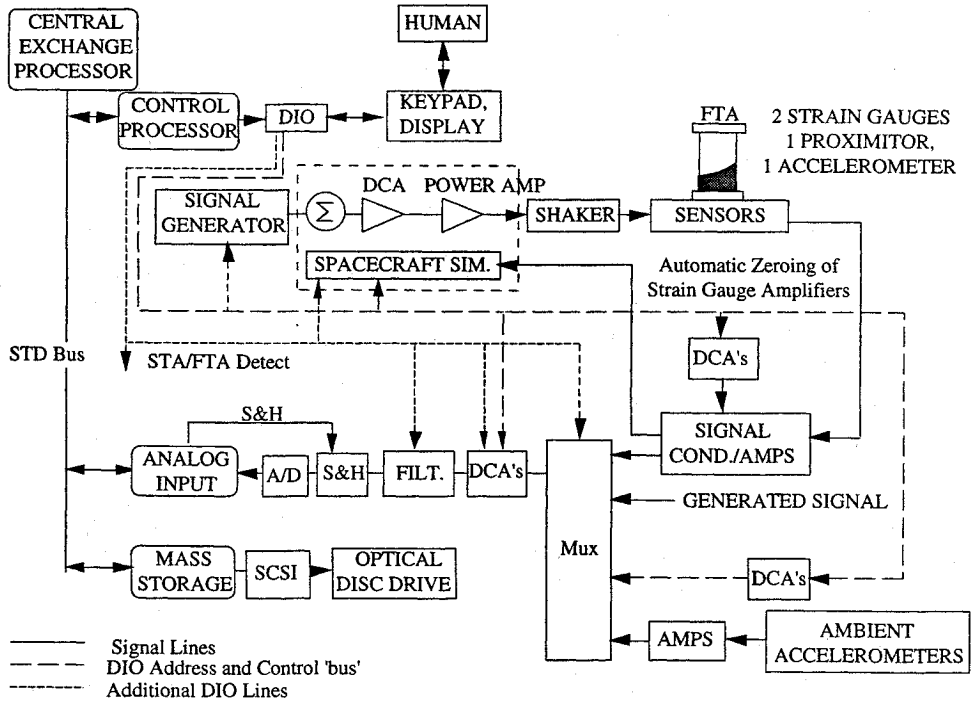

Fig. 1 Schematic of the MODE hardware.

Hardware and Test Procedure

Hardware Description

The MODE hardware as used in the fluid slosh experiments consisted of the experimental support module (ESM), shaker and force-balance assembly, and the fluid test articles (FTAs).[11] The functional objective for the MODE hardware was to establish on the shuttle middeck a small dynamics laboratory with which the forced response of various systems could be determined. The core of this laboratory is the MODE ESM. The ESM has a computer, a 16-key keyboard, an alphanumeric display, a 200-MB WORM disk for storage, 64 digital input and output (DIO) lines, and 16 analog-to-digital (A/D) channels. The ESM has excitation, data storage, signal conditioning, and experiment control functions, and can be used with various types of dynamic test articles.

Figure 1 is a schematic of the MODE hardware. Both the fluids and structural experiments are controlled by the ESM. Upon power-up the astronaut can select a prestored protocol, which contains the desired forcing amplitude, duration, and frequency information for each specific experiment. Given a forcing amplitude and frequency, the ESM generates the appropriate sinusoidal excitation signal. For fluid slosh experiments, this signal is fed via a power amplifier to an electromechanical shaker, to which a very sensitive force balance is attached (Table 1 and Fig. 2). This force balance can measure slosh forces in both the planar (x) and nonplanar (y) directions. The frequency response of the fluid is determined by sinusoidal dwell testing. The experimental control function allows for the sinusoidal excitation frequency to be smoothly increased or decreased, i.e., changed without loss of phase continuity. In addition to the measurement of the slosh forces, the displacement and acceleration of the tank in the x direction are also measured, as are the ambient accelerations. The fluid slosh behavior was also recorded by a video camcorder.

The FTAs containing the fluids under investigation are attached to the force balance via a quick-release coupling. Since the experiment design calls for the fluid to be aligned in the bottom of the tank, this coupling enables the astronauts, after having aligned the fluid, to attach the tank to the force balance without disturbing the alignment. Alignment of the fluid is required at the start of a new experiment or when unanticipated realignment occurs.

A unique feature of the MODE hardware is that the force balance and accelerometer signals are automatically zeroed by the ESM.[11] This avoids signal saturation due to thermal drifts. The digitally controlled amplifiers (DCAs) in the signal paths also enable researchers to select optimal signal gains to insure the best possible signal-to-noise ratios and to avoid channel saturation. The sensitivities of the measured signals at an amplifier gain of unity are summarized in Table 1. By using the DCAs, each of these sensitivities can be amplified by as much as 16 times.

Table 1 FTA sensor and balancing sensitivities

Measurement	Symbol	Sensitivity
Planar slosh force	K_{Fx}	20.90 V/N
Nonplanar slosh force	K_{Fy}	21.51 V/N
Displacement	K_x	0.327 V/mm
Acceleration	K_{ax}	0.78 V/m-s^{-2}

The MODE hardware allows the investigation of both the uncoupled behavior of a fluid and the coupled behavior of a fluid-spacecraft system.[1] In the uncoupled configuration, a commanded displacement signal directly drives the motion of the electromechanical shaker. In the coupled configuration, the force excitation signal is fed to an analog simulation of a spacecraft lateral mode (Fig. 3). The analog simulation is also fed a signal that represents the measured slosh force, i.e., the total force measured by the reaction balance minus the dry force component. The calculated spacecraft displacement is then commanded of the shaker. In both the uncoupled and coupled configurations, a shaker servo loop insures that the commanded displacement is tracked within 2% in amplitude and 5 deg in phase. The parameters of the simulated spacecraft mode (i.e., frequency, damping ratio, mass, and dry mass component) are stored in the protocols and are digitally set with the ESM's DIO lines.

Fluids and Tank Geometries

The selection of the test fluids was driven by the following criteria: the fluids had to be safe, and for engineering relevance their properties had to match those of typical spacecraft propellants (Table 2). Given these criteria, silicone oil with 5-cs viscosity was selected as the primary test fluid. This silicone oil is nontoxic and nonflammable, and it approximately matches the properties of liquid oxygen. However, the free-surface stability of the silicone oil was a concern. Given the proven free-surface stability of water, triply distilled water was selected as the secondary test fluid. The properties of the silicone oil and of water are also presented in Table 2.

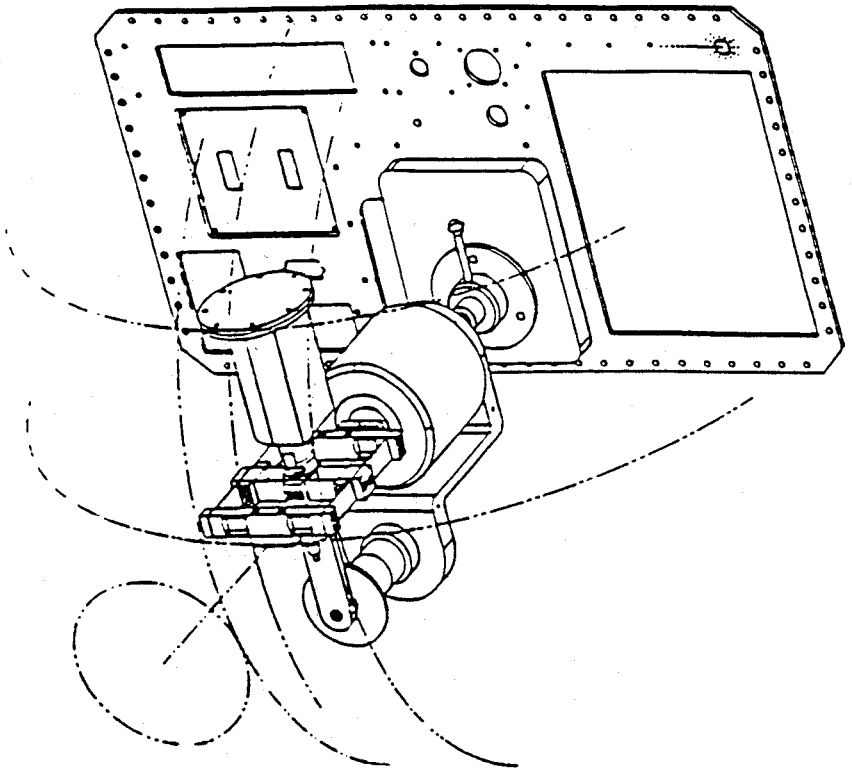

Fig. 2 Line drawing of the MODE FTA force balance.

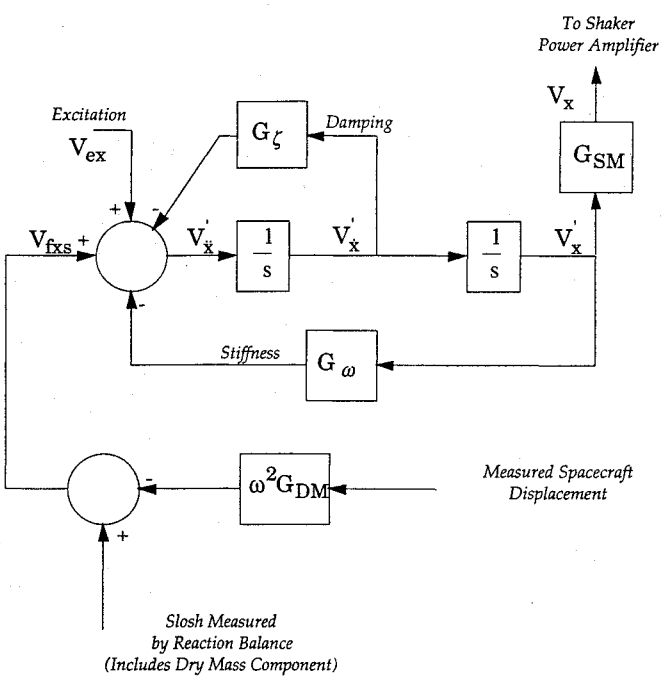

Fig. 3 Analog simulation of a spacecraft's lateral mode.

The geometry of the fluid test article was selected so that the results could be extrapolated to typical space storage tanks. A cylindrical tank with a flat bottom and a cylindrical tank with a spherical bottom were chosen. A variety of existing ground experimental results were available on these tank shapes to support design and analysis.

In sizing the tanks, an important criterion was that the equilibrium free surface of the fluid must be retained during all Space Shuttle maneuvers except primary RCS firings. The following equation gives the critical negative acceleration at which the free surface will lose stability and reorient:

$$g_{\text{reor}}^{\text{crit}} = \frac{(-3.4 + 2.6\cos\alpha)\sigma}{\rho a^2} \tag{1}$$

Table 2 Fluid properties

Fluid	Density ρ, kg/m^3	Kinematic Viscosity ν, cm^2/s	Surface tension σ, dyne/cm
Liquid H_2	70.0	0.00197	1.9
Liquid O_2	1140.0	0.0017	13.2
Hydrazine	1010.0	0.0097	63.2
Silicone oil	920.0	0.0500	19.7
Dist. water	998.0	0.0100	72.8

An evaluation of the ambient and operational accelerations onboard the Space Shuttle resulted in a requirement that the contained fluid must withstand at least $7 \times 10^{-3} g$ of negative acceleration before realignment.

A second criterion that governed the selection of the tank size was a minimum slosh frequency of 0.5 Hz. A slosh frequency much below this would require extremely long testing times and place severe requirements on the sensitivity of the acceleration and forcing/sensing elements. A 3.1-cm-diam tank satisfied both the free-surface stability and minimum-slosh-frequency requirements. The decision to use 3.1-cm-diam tanks was further justified by the fact that a multitude of ground experimental results were already available for tanks of this diameter. The two cylindrical model tanks, one with a flat bottom and one with a spherical bottom, are depicted in Fig. 4.

Test Procedures and Data Reduction

The fluid response data were obtained by sine dwell over a range of frequencies, and for the different force levels. Typical frequency sweeps contained 65 frequency points and dwell times of 6 to 40 s. The excitation window ranged from 50% below the first natural slosh frequency to 2 times that frequency. The signal sampling rate for both the ground and space experiments was 50 Hz, with the antialiasing filters set at 18 Hz.

In postprocessing the results, the time traces of force, displacement, and acceleration were read from the WORM disks, and the harmonic frequency information was extracted from these signals. This retrieval process was repeated for each forcing frequency and amplitude test point. The linear modal characteristics of the contained

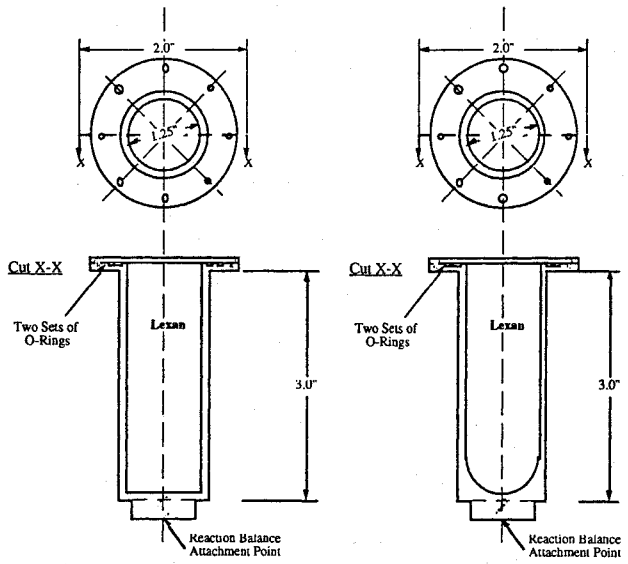

Fig. 4 MODE FTA cylindrical flat- and spherical-bottom tanks.

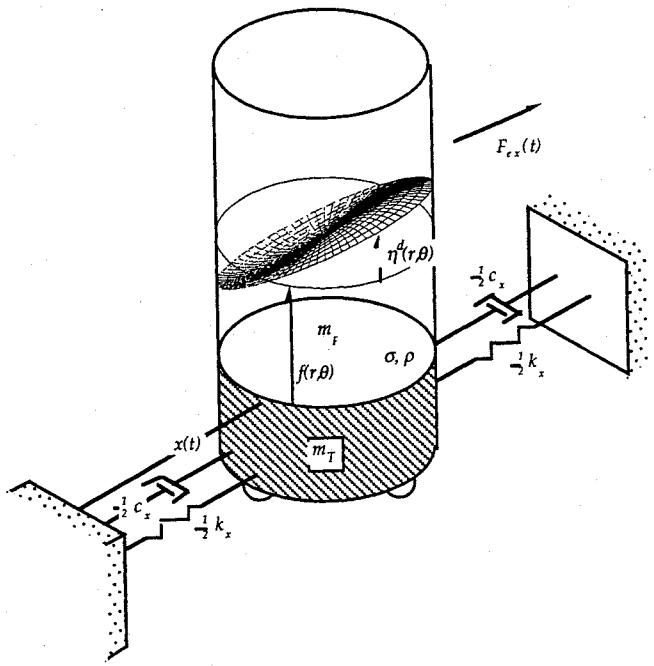

Fig. 5 Fluid-spacecraft study model of a contained fluid.

fluids were determined by fitting a two-complex-pole approximation to the "linear" (lowest forcing amplitude) uncoupled displacement-to-planar-force transfer function. The following is a linearized model of the fluid's first slosh mode:

$$F_{xs} = \ddot{x}m_f - \ddot{q}_1\lambda m_f$$
$$\ddot{q}_1 + 2\zeta_{q_1}\omega_s\dot{q}_1 + \omega_s^2 q_1 = -\ddot{x} \tag{2}$$

The modal parameters λ, ζ_{q_1} and ω_s are obtained from the complex-pole fit.

The frequency-domain transfer functions from displacement to planar slosh force and from displacement to nonplanar slosh force were also obtained for the uncoupled tests. In the coupled tests, the transfer functions from excitation force to tank displacement were also obtained for the different excitation amplitudes.

Modeling

Nonlinear Fluid Phenomena

Because the scientific objective of MODE is to understand the coupled nonlinear slosh of fluids in microgravity, an appropriate nonlinear model was developed at MIT to compliment the experimental program.[1] A complete description of the model and its correlation with ground and flight data is beyond the scope of this article, but a summary of the major sources of nonlinearities in contained fluids and the major differences between the one-gravity (earth) and microgravity (space) dynamic behavior of fluids is outlined, as is the model derivation. The section concludes with a summary of linearized fluid slosh models with which the linear low-slosh-amplitude modal behavior of contained fluids can be predicted, and which will be used for experimental correlation.

Figure 5 is a schematic representation of a contained fluid in a flat-bottom cylindrical tank. The springs and dashpots are a mechanical representation of a spacecraft attitude control mode or a flexible mode. In this model, the free surface is described by the sum of two two-dimensional functions: $f(r, \theta)$, the equilibrium free-surface height, and $\eta_d(r, \theta)$, the dynamic perturbation from this equilibrium. The internal flow can be described by a three-dimensional potential function ϕ. The two major contributions to the nonlinear dynamic behavior of the contained fluid and the influence of gravity on these contributions are outlined in the next two sub-subsections.

Time-Dependent Free-Surface Boundary Condition

The relationship between the fluid flow potential function and the free-surface function is one of the major sources of nonlinearities in the fluid slosh behavior for finite motion.[1,12–14] Consider the action of the convection forces at the free surface of the fluid. The potential flow and the free-surface motion η must satisfy the kinematic boundary condition:

$$\frac{\partial \eta}{\partial t} + \nabla\phi \bullet \nabla\eta\,|_{z=\eta} = \left.\frac{\partial \phi}{\partial z}\right|_{z=\eta} \tag{3}$$

This equation is an analytical expression of the Dirichlet and Neumann problems and constitutes a nonlinear relation between the fluid flow potential and the free-surface motion. The effects of a change in the ambient acceleration (gravity) can be better revealed when free-surface motion is expressed in terms of the equilibrium free surface (f) and the dynamic motion of the free surface (f), that is,

$$\eta = f + \eta^d \tag{4}$$

Using Eq. (4), Eq. (3) can be written as

$$\frac{\partial \eta^d}{\partial t} + \nabla\phi \bullet \nabla(f + \eta^d)\,|_{z=\eta} = \left.\frac{\partial \phi}{\partial z}\right|_{z=\eta} \tag{5}$$

From this equation it is clear that the nonlinear free-surface boundary condition is a function of the equilibrium free surface. The equilibrium free surface is strongly dependent on gravity, as can be seen by examining Fig. 6, an analytical prediction of the equilibrium free surface under one- and zero-gravity conditions. One can conclude that the nonlinear effects of the free-surface boundary condition will change between one-gravity and microgravity conditions.

Capillary Potential Energy

Another source of nonlinearities is the potential energy associated with the capillary forces,[15–17]

$$U_\sigma = \sigma \iint_S \sqrt{1 + \nabla\eta \bullet \nabla\eta}\,\mathrm{d}S \tag{6}$$

The potential energy of the free surface is a function of the total dynamic free-surface area, which is a complex nonlinear function of the free-surface shape η. Using Eq. (4), it can be shown that the capillary energy is also a function of the equilibrium free surface, that is,

$$U_\sigma = \sigma \iint_S \sqrt{1 + \nabla(f + \eta^d) \bullet \nabla(f + \eta^d)}\,\mathrm{d}S \tag{7}$$

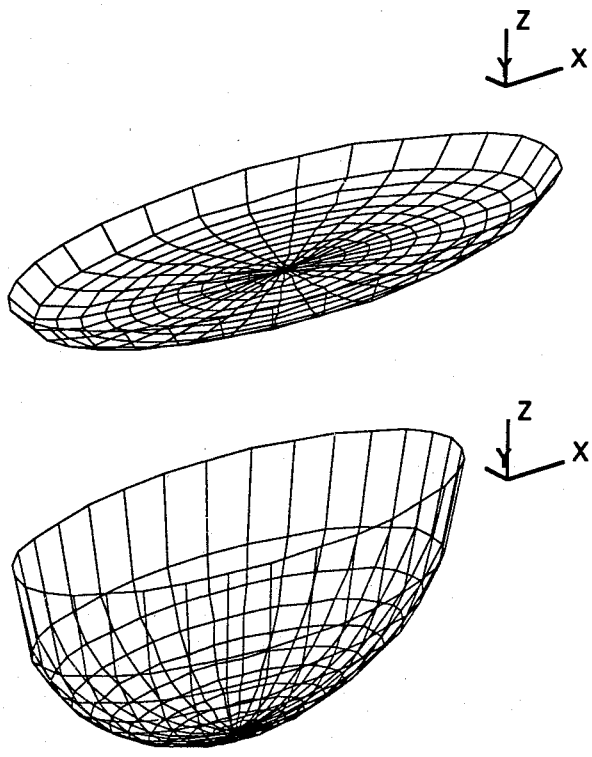

Fig. 6 Predicted equilibrium fluid free surface for silicon oil on earth and in space (cylindrical tank, diam = 3.1 cm, contact angle $\alpha = 1$ deg).

The shape of the equilibrium free surface is a function of the Bond number, a nondimensional measure of the relative importance of gravity vs capillary forces:

$$Bo = (\rho g a^2/\sigma) \tag{8}$$

On earth gravity forces dominate, whereas in space the equilibrium free surface is determined largely by the surface-tension forces. Gravity tends to minimize the free-surface height, and the capillary forces (given the required contact angle) tend to minimize the free-surface area. Note that, because of gravity gradients, moderate Bond numbers can exist in space, especially for larger tanks and spacecraft.

Linearized Models

For very small slosh amplitudes, linearized models[1,15] can be used to describe the fluid slosh dynamics. This section summarizes the linear models with which the natural frequency and damping ratio of the fluid can be predicted. The MODE ground and space experimental results will be used to determine the accuracy of these models for one-gravity and microgravity conditions.

For an inviscid fluid in a flat-bottom cylindrical tank, with its contact angle free to move, the following is an approximate equation for the first slosh frequency ω_s:

$$\omega_s = \left[\frac{\sigma}{\rho a^3}\tanh\left(1.84\frac{h}{a}\right)(6.26 + 1.84\,Bo - 4.76\cos\alpha)\right]^{\frac{1}{2}} \tag{9}$$

Note that this equation is not valid for fluids that exhibit contact-angle hysteresis and that, in general, contact-angle hysteresis tends to increase the natural slosh frequency. A more complex model, which includes the first-order effects of contact-angle hysteresis, is presented in Ref. 17 but requires numerical solution.

The major effect of capillary viscous forces is on the amount of energy dissipated (damping) by the fluid motion. These dissipative effects are important because the orbital lives of most satellites are determined by the fuel expenditure required to control the nutational stability of the spacecraft. The fuel expenditure is proportional to the energy dissipated by the capillary viscous forces and other nonconservative forces.

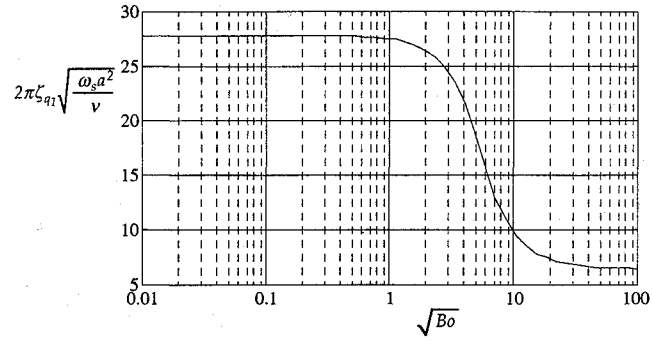

Fig. 7 Modal damping ratio as a function of Bond number.[18]

Although some analytical scaling analysis and estimation are possible,[18–21] the prediction of fluid damping relies heavily on the results of previous experiments. At high Bond numbers ($Bo > 10$), the damping of the free-surface waves scales with gravity and viscosity in a nondimensional parameter similar to the Reynolds number:

$$N_{\nu_1} = \frac{\nu_K}{\sqrt{ga^3}} \tag{10}$$

When gravity approaches zero, this parameter is not the proper scaling, for it would imply that the fluid becomes infinitely damped under microgravity conditions. When Eq. (10) is multiplied by the square root of the Bond number [Eq. (8)], an alternative scaling parameter is obtained:

$$N_{\nu_2} = \nu_K\sqrt{\frac{\rho}{\sigma a}} \tag{11}$$

The multiplication of Eq. (10) by $\sqrt{Bo}$ is equivalent to scaling the Navier–Stokes equations using surface tension instead of gravity forces as a reference. Salzman and Masica[18] experimentally obtained slosh damping ratios for fluids in a bare-wall cylindrical tank using drop-tower tests. These experiments predict the slosh damping ratio as a function of Bond number as shown in Fig. 7.

Test Results

Test Matrix Selection

The matrix of the test actually conducted on orbit is shown in Table 3, and a far more extensive test matrix was completed on the ground. Since the MODE precursor flight indicated that silicone oil presented a possible free-surface equilibrium stability problem, that fluid was tested only in the uncoupled configuration. For the coupled tests, the spacecraft model parameters (frequency ratio $\nu = 1.04$ and mass ratio $\mu = 0.15$) were selected to yield the highest possible fluid-to-spacecraft dynamic coupling. The damping ratio ζ of the spacecraft's mode was set to 5% of critical. Table 3 also summarizes the tank fill levels and fluid masses associated with each of the different tests in the space test matrix.

The forced-response characteristics for all the fluids and tanks were determined by using three logarithmically spaced forcing amplitudes. Increasing excitation-frequency sweeps were used at all the forcing amplitudes. A additional sweep, with the excitation frequency decreasing from one test point to the next, was also performed at the highest forcing amplitude. The excitation displacement amplitudes for the uncoupled tests were $x_{ex}/d = 0.32\%$, 1.02%, and 3.22%. The forcing excitation amplitudes for all the coupled tests were chosen so that below resonance the displacement response would be comparable to that in the uncoupled tests. For the ground tests, the forcing amplitudes were $F_{ex} = 1.35$, 4.27, and 13.51 mN. The excitation amplitudes for all the space coupled tests were $F_{ex} = 0.346$, 1.095, and 3.46 mN.

Figures 9–28 present the ground and space results for all the cases in the test matrix (Table 3). In these figures, each symbol represents the harmonic component as measured for that forcing amplitude and frequency. Table 4 presents a legend for the symbols used in these

Table 3 Space test matrix

Fluid	Tank bottom	Test type	Fluid mass mf, g	Fluid depth h, mm
Si oil	Flat	Uncoupled	19.10	27.51
Si oil	Sph.	Uncoupled	16.02	28.24
Water	Flat	Uncoupled	23.42	31.00
Water	Sph.	Uncoupled	19.51	31.00
Water	Flat	Coupled	23.42	31.00
Water	Sph.	Coupled	19.51	31.00

Table 4 Symbols used in Figs. 9–28

Forcing amplitude	Direction of change in forcing frequency	Symbol
Low	Increasing	+
Medium	Increasing	*
High	Increasing	×
High	Decreasing	o

Table 5 Silicone oil: measured and predicted linear modal parameters

		1st slosh frequency f, Hz		Damping ratio ζ,%		Mass frac. λ
Tank	Test	Pred.	Meas.	Pred.	Meas.	Meas.
Flat	Earth	5.19	5.24	3.93	4.0	0.24
Flat	Space	0.49	0.68	37.5	36.3	0.24
Sph.	Earth	5.19	5.26	3.93	4.2	0.22
Sph.	Space	0.49	0.65	37.5	39.1	0.33

graphs. In order to facilitate the comparison of the ground and space results, the ground transfer functions are followed by the results of the equivalent space test. In the next two subsections, the ground and space results are discussed separately and then compared.

Ground Test Results

Silicone-Oil Uncoupled Results

The measured linear modal parameters of the uncoupled silicone-oil tests, as obtained from the complex two-pole fit [Eq. (1)], are summarized in Table 5. For the space results, given the high slosh damping ratios, matching of the phase characteristics was important. The correlation factor for all the fits was better than 95%. The ground Bond number for both of the tank geometries is 110. The predicted slosh frequencies and damping ratios presented in Table 5 are obtained from Eq. (17) and Fig. 7, respectively. Note that it is assumed for both the silicone and water cases that the predicted parameters, which are nominally only valid for a flat-bottom cylindrical tank, can be used as estimates of the modal characteristics of the fluids in the spherical-bottom tanks.

For silicone oil, the measured linear modal frequencies are within 1% of the predicted values, and the measured damping ratios are within 7% of the predicted values. The experimental results (Figs. 9, 11, and 13) show strong amplitude-dependent nonlinear slosh behavior. For the flat-bottom tank, Fig. 9 shows that the first slosh frequency shifts from 5.24 Hz at the lowest forcing amplitude ($x_{ex}/d = 0.32\%$) to 4.6 Hz at the highest forcing amplitude ($x_{ex}/d = 3.2\%$). This is a shift of 12% in frequency. For the spherical bottom tank this shift, from 5.26 to 4.6 Hz (Fig. 13), is also 12%.

When the planar and nonplanar slosh-force response of the fluid in the flat-bottom tank is studied, it is clear that the fluid swirls at the highest forcing amplitude. This swirl motion manifests itself in a second resonance peak, which appears close to the linear slosh frequency (5.26 Hz). Not only does the fluid swirl at this forcing amplitude, but the slosh also has multiple response states. The slosh response is different for up and down frequency sweeps between 5.6 and 6 Hz (Figs. 9, 11, and 13). Depending on whether the forcing frequency is increased or decreased, the fluid motion is either a planar slosh or a nonplanar swirl. This behavior

Table 6 Water: measured and predicted linear modal parameters

		1st slosh frequency f, Hz		Damping ratio ζ,%		Mass frac. λ
Tank	Test	Pred.	Meas.	Pred.	Meas.	Meas.
Flat	Earth	6.26	6.30	3.0	4.7	0.26
Flat	Space	3.18	3.31	6.5	4.4	0.17
Sph.	Earth	6.26	6.40	3.0	5.3	0.24
Sph.	Space	3.18	3.37[a]	6.5	6.5[a]	0.28

[a]Less accurate.

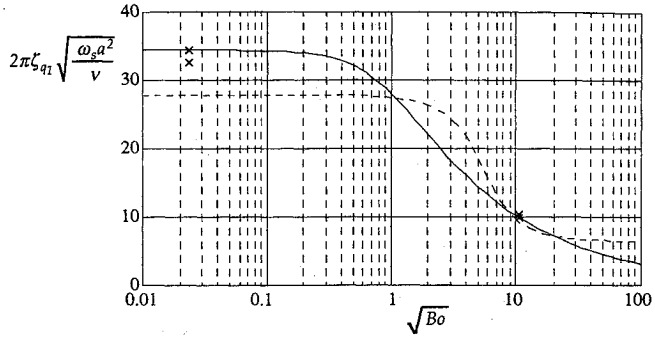

Fig. 8 Comparison of the constant-damping-coefficient model and silicone ground and space damping results. Also plotted is the Salzman and Masica empirical model (dashed line). Measured values are indicated with ×.

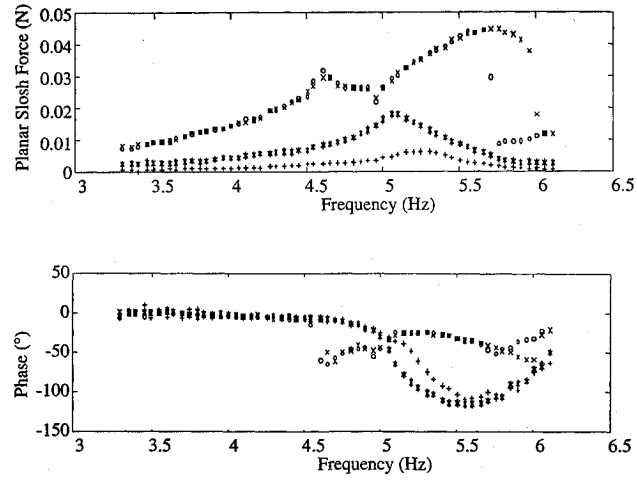

Fig. 9 Uncoupled test on earth with silicone oil in a flat-bottom tank: planar slosh force and phase angle.

is also observed for the silicone oil in the spherical-bottom tank (Fig. 13).

When the slosh behavior of silicone oil in the flat-bottom tank (Fig. 9) and in the spherical-bottom tank (Fig. 13) is studied, the conclusion is that there is no observable difference. From theory it is known that the flow potential ϕ decays exponentially with depth, and it must be concluded that the flow potential near the bottom of the tank is too weak to change the slosh behavior of the fluid.

Water Uncoupled Results

The measured linear modal parameters of the uncoupled water tests are summarized in Table 6. The ground Bond number for both the tank geometries is 34. The predicted slosh frequencies and damping ratios, also presented in Table 6, were obtained from the linear model (with a correction for contact-angle hysteresis[18]) and Fig. 7, respectively. Once the linear model was corrected to include the linear effects of contact-angle hysteresis, the predicted and measured frequencies were within 2.5%. The measured damping ratios are within 33% of the predicted values.

The ground results (Figs. 15, 17, 19, and 21) show strong amplitude-dependent nonlinear slosh behavior. In Fig. 15 the first

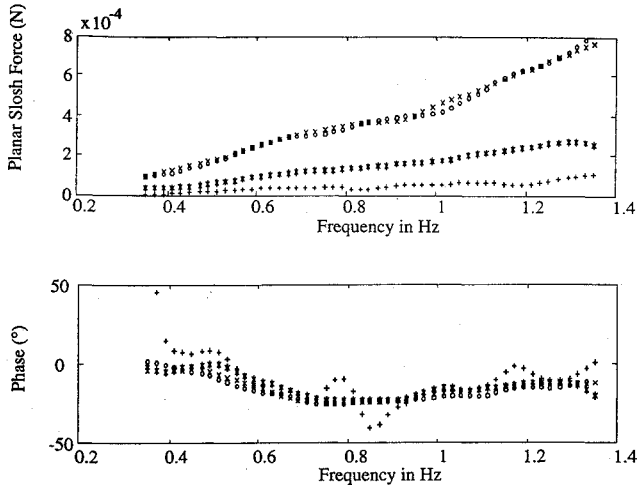

Fig. 10 Uncoupled test in space with silicone oil in a flat-bottom tank: planar slosh force and phase angle.

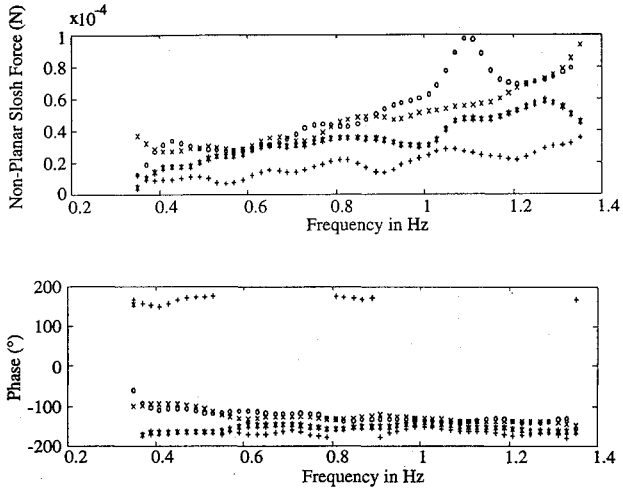

Fig. 12 Uncoupled test in space with silicone oil in a flat-bottom tank: nonplanar slosh force and phase angle.

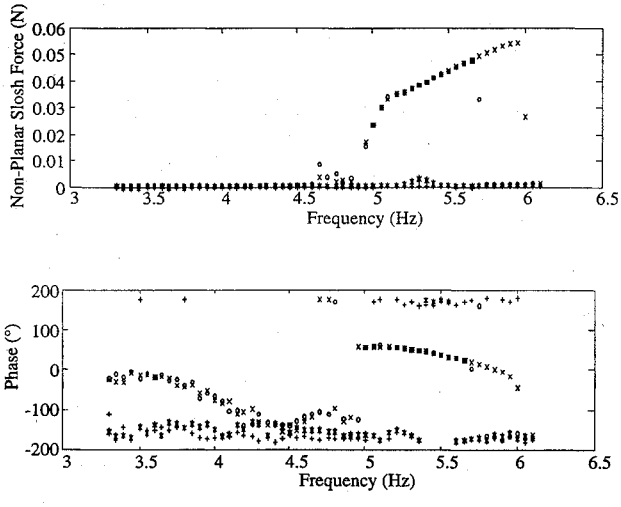

Fig. 11 Uncoupled test on earth with silicone oil in a flat-bottom tank: nonplanar slosh force and phase angle.

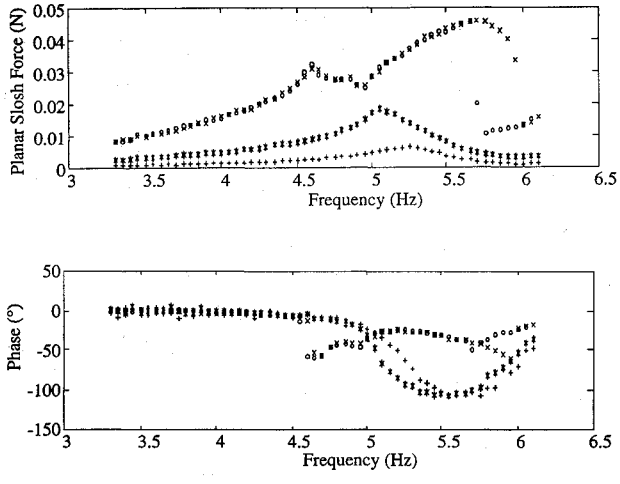

Fig. 13 Uncoupled test on earth with silicone oil in a spherical-bottom tank: planar slosh force and phase angle.

slosh resonance shifts from 6.3 Hz at the lowest forcing amplitude ($x_{ex}/d = 0.32\%$) to 4.95 Hz at the highest forcing amplitude ($x_{ex}/d = 3.2\%$), a shift of 21%. For the spherical-bottom tank this shift, from 6.5 to 5.15 Hz (Fig. 19), is 22%.

Examining the planar and nonplanar slosh-force response, it is clear that the fluid swirls at the higher forcing amplitudes. When the water results (Figs. 15 and 17) are compared with the silicone-oil results (Figs. 9 and 11), it is also evident that this amplitude dependent behavior manifests itself at lower forcing amplitudes in the water experiments. In the water experiments (Figs. 15, 17, 19, and 21) it can be seen that between 5.9 and 6.7 Hz for the intermediate forcing amplitude, and between 5.2 and 7.2 Hz for the highest forcing amplitude, the fluid response is a nonplanar swirl. This swirl motion manifests itself in a second resonance peak, which appears close to the linear planar slosh frequency (6.3 Hz). Not only does the fluid swirl at this forcing amplitude, but the slosh also has multiple response states. The slosh response is different for up and down frequency sweeps between 6.3 and 7.2 Hz (Figs. 15, 17, 19, and 21). Depending on the direction in which the forcing frequency is changed, the fluid motion is either a planar slosh or a nonplanar swirl. Similar behavior was also observed for the water in the spherical-bottom tank.

As with the silicone oil, the results from the flat-bottom tank (Fig. 15) and from the spherical-bottom tank (Fig. 17) show no significant difference, confirming a weak dependence on tank bottom geometry for this fill ratio.

Water Coupled Results

The coupled ground experimental results on water are depicted in Figs. 23, 25, and 27. In Figs. 23 and 27, the lower-frequency resonance peak is the coupled spacecraft mode, and the higher-frequency resonance peak is that of the first fluid slosh mode. The frequencies at which these resonances occur decrease as the forcing amplitude is increased. The spacecraft mode's frequency decreases from 5.9 (lowest forcing amplitude, $x_{ex}/d = 0.32\%$) to 5.3 Hz (highest forcing amplitude, $x_{ex}/d = 3.2\%$), a 10% shift. The frequency of the slosh mode changes from 7.15 to 6.35 Hz, an 11% shift. From Fig. 25 it is clear that the slosh not only is nonlinear but also exhibits nonplanar swirl similar to the nonplanar motion observed in the uncoupled tests. The frequency range over which this nonplanar swirl occurs is roughly from 5.5 to 6.7 Hz. Multiple response states can also be observed between 5.3 and 5.7 Hz (Figs. 23 and 27).

When the uncoupled and coupled results are compared, one can conclude that the filtering effect of the spacecraft mode tends to reduce the nonlinear behavior of the system. But even with this "filtering" it is clear from the results (Figs. 23 to 27) that a linear model would fail to model accurately the dynamic behavior of a coupled fluid-spacecraft system.

Orbital Test Results

Silicone-Oil Uncoupled Results

When the results for the linear parameters for the microgravity fluid tests in Table 5 are studied, it can be seen that the measured linear modal frequencies (0.68 and 0.65 Hz) are approximately 35%

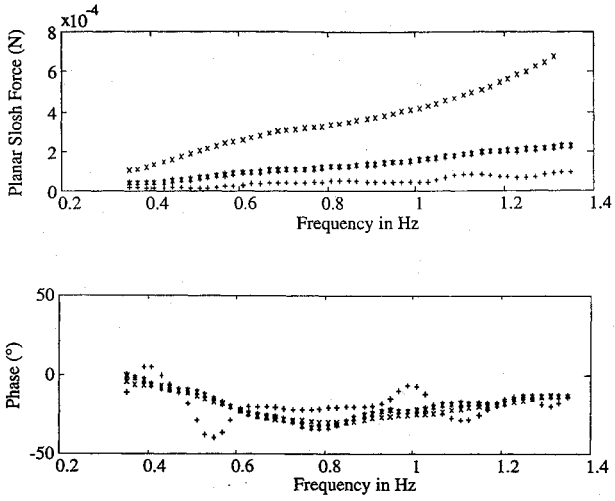

Fig. 14 Uncoupled test in space with silicone oil in a spherical-bottom tank: planar slosh force and phase angle.

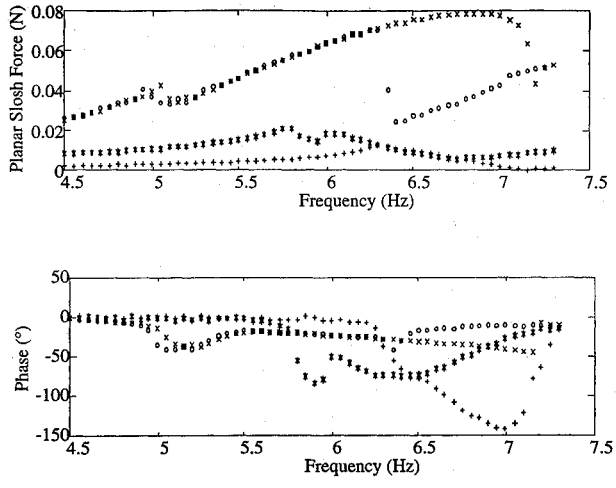

Fig. 15 Uncoupled test on earth with distilled water in a flat-bottom tank: planar slosh force and phase angle.

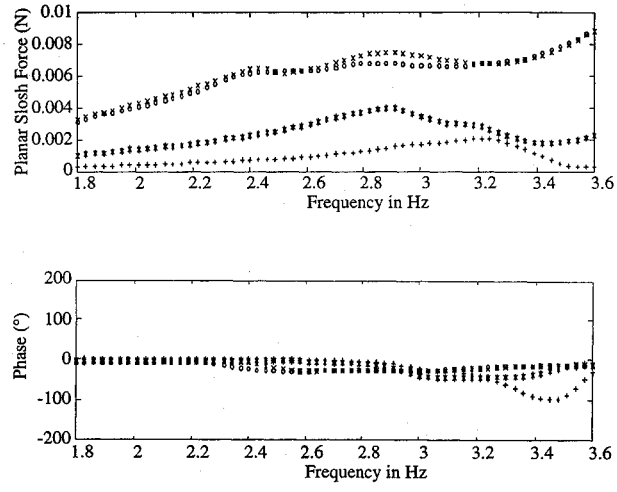

Fig. 16 Uncoupled test in space with distilled water in a flat-bottom tank: planar slosh force and phase angle.

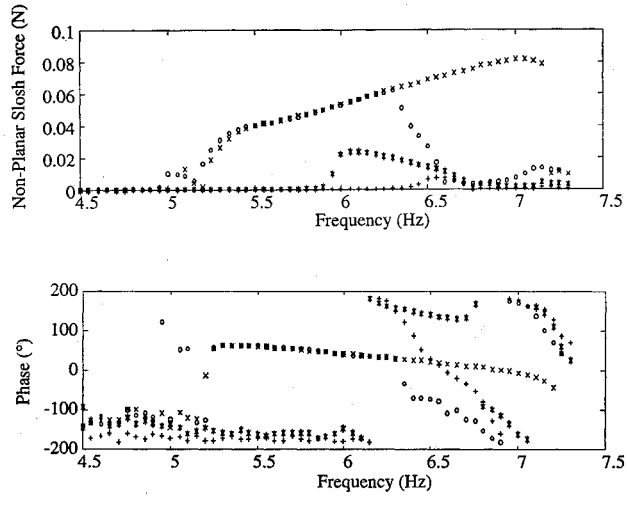

Fig. 17 Uncoupled test on earth with distilled water in a flat-bottom tank: nonplanar slosh force and phase angle.

higher than the frequencies predicted by the linear model. As with the ground experiments, the measured damping ratios are within 7% of the predicted values. The difference may be explained by noting that Fig. 7 was obtained from slosh decay measurements. A phenomenon that is often ignored is that although free-decay tests do measure energy dissipation, the action of nonlinear forces transfers energy between modes (normally from lower to higher modes, which have higher energy dissipation rates). Thus the measured decay rate is not a true measurement of the energy dissipated (damping) in the excited mode, but rather of the total energy dissipated in the slosh motion.

Studying Figs. 10, 12, and 14, it can be concluded that the silicone-oil slosh dynamics are essentially linear and planar in space. The high energy dissipation in the on-orbit tests reduces the slosh modal amplitudes and thus the amplitude-associated nonlinear behavior. One may expect the higher forcing amplitudes will result in nonlinear slosh behavior, but from the MODE video observations it is believed that higher forcing amplitudes may actually cause the fluid to slosh around the top of the tank.

When the slosh behavior of the silicone oil in the flat-bottom tank (Fig. 10) and in the spherical-bottom tank (Fig. 14) is studied, the conclusion is that there is, as with the ground experiments, no observable difference in the behavior.

Water Uncoupled Results

The linear parameters of the on-orbit water tests are listed in Table 6, and the frequency responses are shown in Figs. 16, 18, 20, and 22. Unfortunately, the frequency excitation window for the spherical-bottom tests (Figs. 20 and 22) was not centered around the first planar-slosh natural frequency. The space experiments failed to completely capture the linear (low-amplitude) slosh characteristics, but valuable data were still obtained for the higher forcing amplitudes. The modal characteristics for this case (marked with a footnote in Table 6) are of lower accuracy than the other measured parameters. Considering both the flat- and spherical-bottom tanks, the agreement between the predicted and measured natural frequencies (within 6%) and the damping ratios (within 48%) must be considered acceptable. Recall that the model used for the frequency prediction included the linear effects of contact-angle hysteresis.

For the flat-bottom tank, the natural frequency changes from 3.3 Hz at the lowest forcing amplitude to 2.4 Hz at the highest forcing amplitude, a 27% shift. The results on the planar slosh force (Fig. 16) show the same double resonance observed in the ground experiments: the first peak, around 2.4 Hz, is interpreted as the shifted nonlinear planar-slosh frequency, and the second is associated with the swirl motion that occurs close to the linear planar-slosh frequency (3.3 Hz). Swirl is clearly evident when results on the nonplanar-slosh force are studied (Fig. 18). The transition to the swirl motion is smooth. Multiple response states, dependent on the direction in which the forcing frequency is changed, are observed between 2.6 and 3.15 Hz (Figs. 16 and 18).

Despite the less than optimal frequency window for the spherical-bottom tank, one can conclude from Figs. 16 and 20, as well as

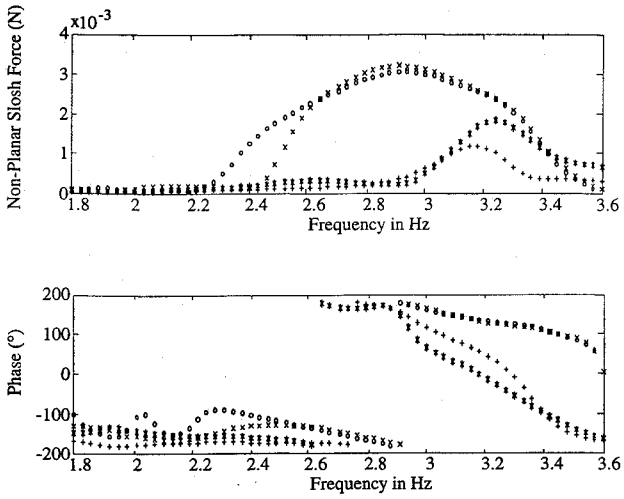

Fig. 18 Uncoupled test in space with distilled water in a flat-bottom tank: nonplanar slosh force and phase angle.

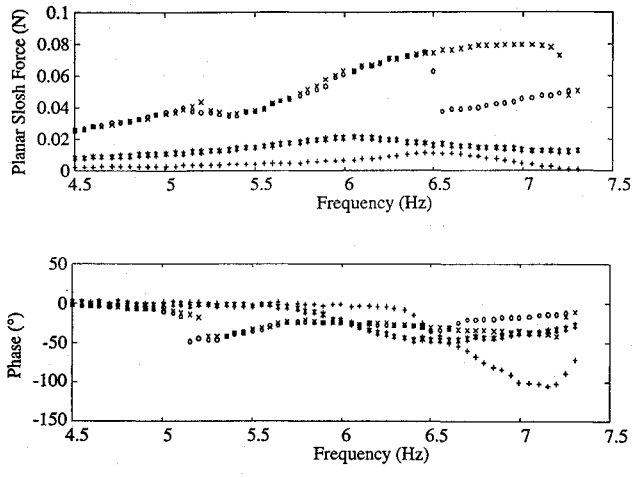

Fig. 19 Uncoupled test on earth with distilled water in a spherical-bottom tank: planar slosh force and phase angle.

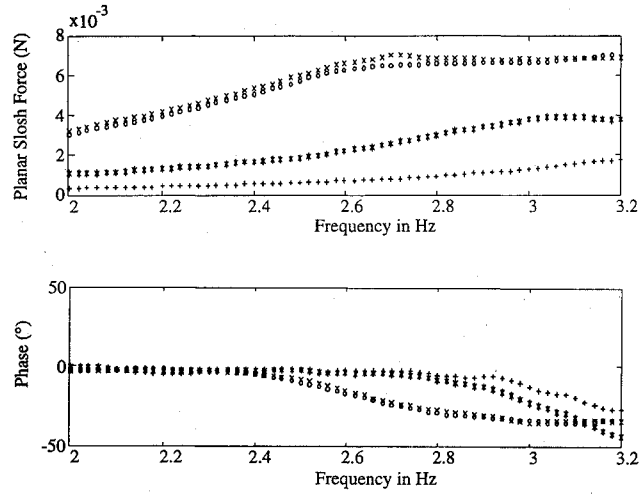

Fig. 20 Uncoupled test in space with distilled water in a spherical-bottom tank: planar slosh force and phase angle.

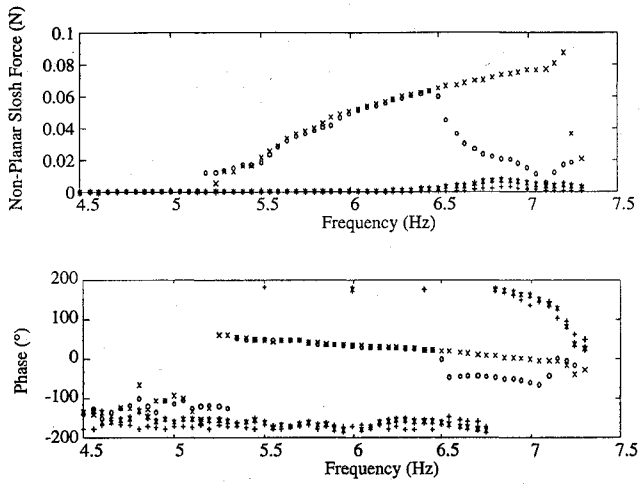

Fig. 21 Uncoupled test on earth with distilled water in a spherical-bottom tank: nonplanar slosh force and phase angle.

18 and 22, that the fluid behavior is qualitatively similar in the flat- and the spherical-bottom tank, but larger quantitative differences are present than in the silicone results and water ground results.

Water Coupled Results

The water coupled on-orbit experimental results for the flat-bottom tank are depicted in Figs. 24, 26, and 28. The frequency window used for the coupled tests on the spherical-bottom tank (not shown) again failed to capture the fluid resonance for the lowest forcing amplitude.

In Figs. 24 and 28, the lower-frequency resonance peak is the coupled spacecraft mode, and the higher-frequency resonance peak is that of the first fluid slosh mode. The frequencies at which these resonances occur decrease as the forcing amplitude is increased. The spacecraft mode's frequency decreases from 2.82 Hz (lowest forcing amplitude, $x_{ex}/d = 0.32\%$) to 2.6 Hz (highest forcing amplitude, $x_{ex}/d = 3.2\%$), an 8% shift. The frequency of the slosh mode changes from 3.6 to 3.13 Hz, a 13% shift. At the highest forcing amplitude, multiple response states can also be observed between 2.55 and 3.0 Hz (Figs. 24 and 28). From Fig. 26 it is also clear that the slosh exhibits swirl similar to the nonplanar motion observed in the ground tests. The frequency range over which this nonplanar swirl occurs is roughly from 2.5 to 3.6 Hz.

From the space results it can be observed that the nonlinear behavior has been moderated by the presence of the spacecraft mode, similar to what was observed in the ground results.

Comparison of Ground and Space Results

Silicone-Oil Uncoupled Tests

The overwhelming difference between the ground and space results for the silicone-oil tests is the sharp increase in the modal damping ratio on orbit. While a frequency shift of 12% was observed in the ground tests (Figs. 9 and 13) between the lowest and highest forcing amplitude, almost no shift was observed in the space results. (Figs. 10 and 14). Multiple solutions and swirl behavior are also absent in space. The linearizing influence is due to the high slosh damping ratio in space, which effectively limits the amplitude of response and suppresses amplitude-dependent non-linearities.

The very high space damping ratio, as predicted by Fig. 7, can be explained in terms of the fluid slosh-force mechanisms. In space, the dominant restoring force (stiffness) is the weak capillary surface tension, whereas on earth it is gravity. The sharp drop in restoring force results in a drop in the slosh natural frequency from 5.24 Hz on earth to 0.68 Hz in space. However, the fluid slosh damping mechanism (the nonconservative action of the capillary viscous forces in the Stokes layer) is not significantly altered by the presence or absence of gravity. Keeping these mechanisms in mind and studying the equation of a second-order system,

$$M\ddot{q} + D\dot{q} + Kq = F$$
$$\ddot{q} + 2\zeta\omega\dot{q} + \omega^2 q = \frac{F}{M} \tag{12}$$

one can conclude that if the damping coefficient remains constant as the frequency decreases, the damping ratio must increase, as was

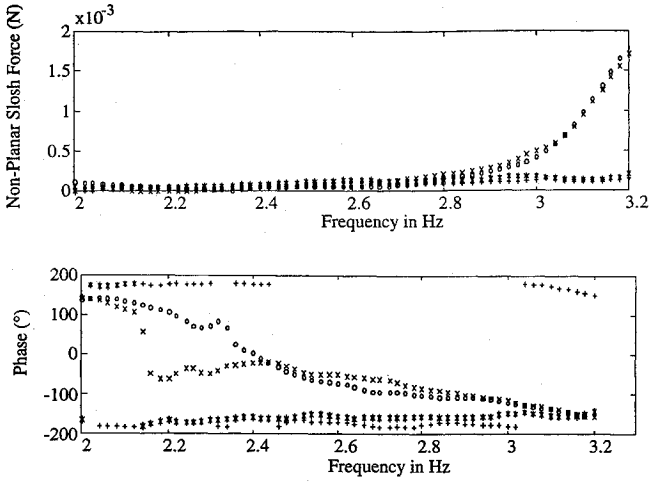

Fig. 22 Uncoupled test in space with distilled water in a spherical-bottom tank: nonplanar slosh force and phase angle.

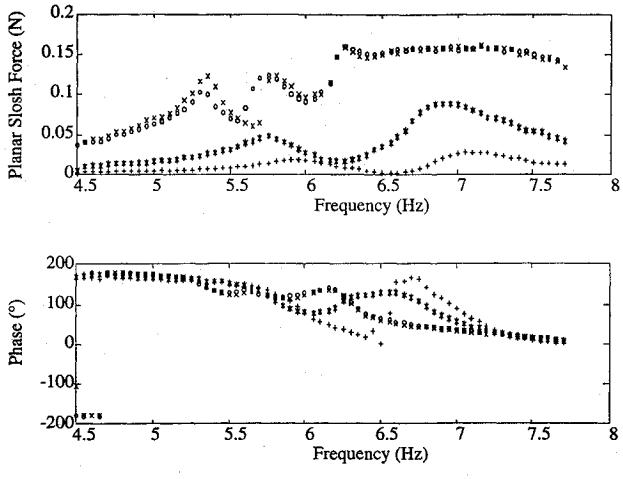

Fig. 23 Coupled test on earth with distilled water in a flat-bottom tank: planar slosh force ($\mu = 0.15, \zeta = 0.05, \nu = 1.04$).

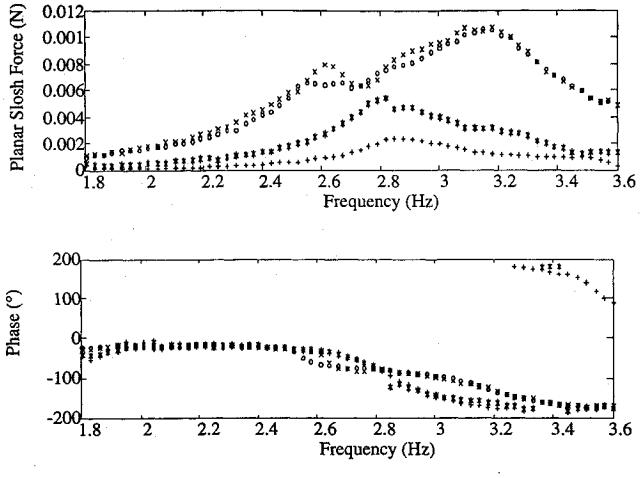

Fig. 24 Coupled test in space with distilled water in a flat-bottom tank: planar slosh force ($\mu = 0.15, \zeta = 0.05, \nu = 1.04$).

observed in the data. Said another way, if the changes in the nonconservative action of the capillary viscous forces are minor, the product of the frequency and damping ratio should be invariant to the change from earth to orbit for a given tank size/geometry. The earth and space products differ by only 15% (Table 5), confirming that the change in restoring force does not fundamentally alter the loss mechanism. This is an important observation in that it implies that space slosh damping ratios can be well estimated from extrapo-

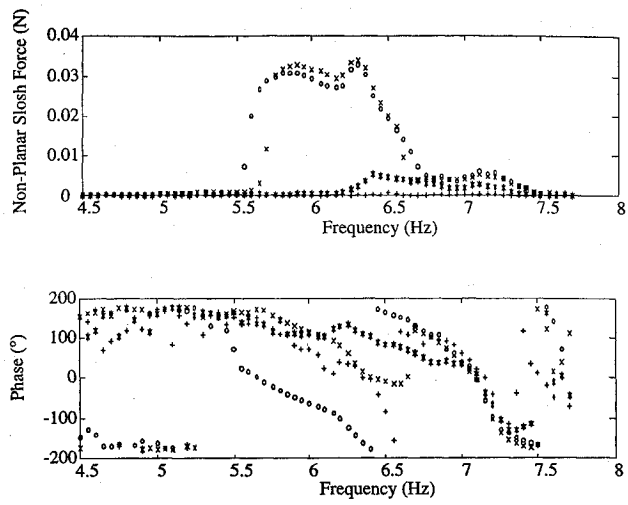

Fig. 25 Coupled test on earth with distilled water in a flat-bottom tank: nonplanar slosh force ($\mu = 0.15, \zeta = 0.05, \nu = 1.04$).

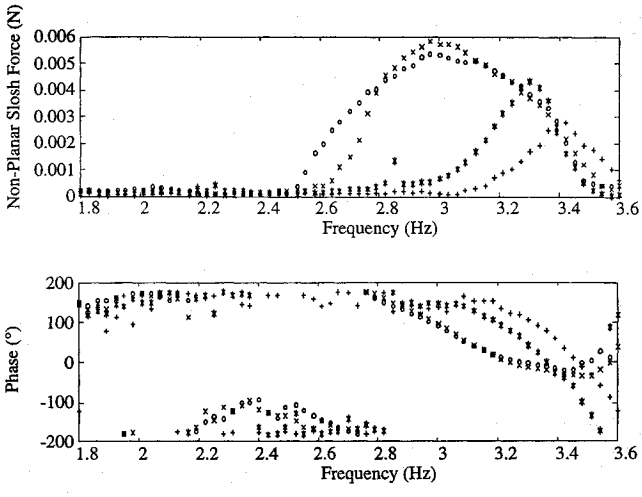

Fig. 26 Coupled test in space with distilled water in a flat-bottom tank: nonplanar slosh force ($\mu = 0.15, \zeta = 0.05, \nu = 1.04$).

lated ground-measured damping ratios. The model predicted by this mechanism is overplotted on the results of Salzman and Masica in Fig. 8.

Water Uncoupled Tests

Both the ground and space results exhibit strong nonlinear and nonplanar slosh characteristics. Some aspects of the response are slightly more nonlinear in space, and some more nonlinear on the ground. In space, when the forcing amplitude is changed from the lowest amplitude to the highest, the shift in resonant frequency (Fig. 16) is 27%. In the ground experiments, for the same change in forcing amplitude the shift is 22%. In contrast, when Figs. 17 and 18 are compared, it is evident that the onset of the swirl is more gradual in space than on earth, and multiple solutions and jumps are less evident. By comparison with the silicone-oil results, the qualitative nature of the nonlinearity is retained in the on-orbit results.

The decrease in the first slosh frequency between ground and space (Table 6) is much smaller for water than the decrease observed in the silicone-oil experiments (Table 5). The explanation for this trend is the influence of contact-angle hysteresis. The first-order effect of contact-angle hysteresis is to increase the slosh frequency, and since contact-angle hysteresis is not a function of the ambient acceleration, the frequency change is smaller when gravity is removed. It can be inferred that in space the contact-angle hysteresis dominates the restoring force, keeping the frequency high, the damping ratio low, and the nonlinearity present.

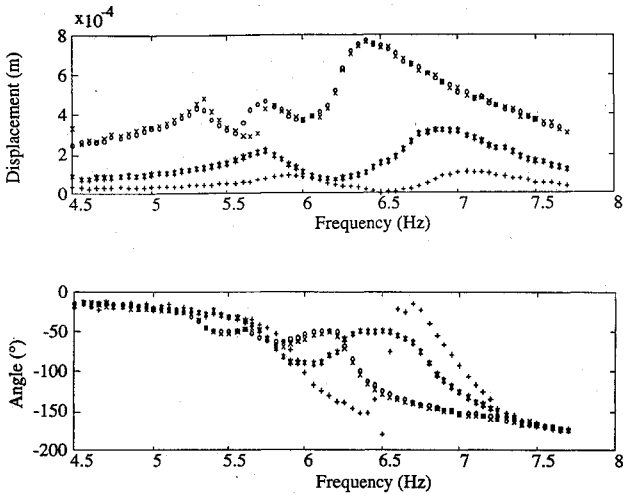

Fig. 27 Coupled test on earth with distilled water in a flat-bottom tank: tank displacement ($\mu = 0.15, \zeta = 0.05, \nu = 1.04$).

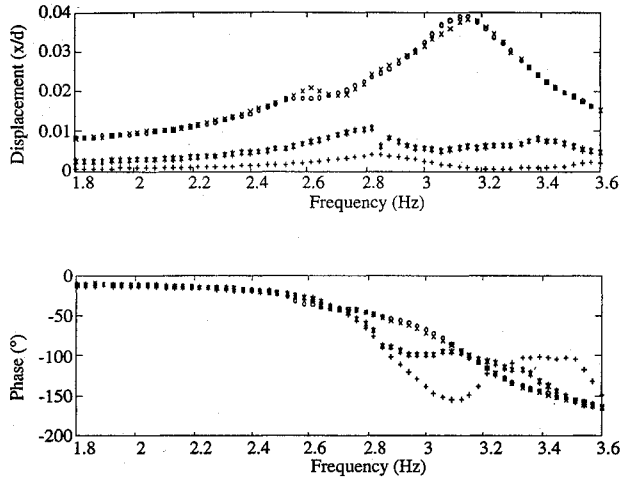

Fig. 28 Coupled test in space with distilled water in a flat-bottom tank: tank displacement ($\mu = 0.15, \zeta = 0.05, \nu = 1.04$).

Water Coupled Tests

The water coupled experimental results (Figs. 24, 26, and 28) clearly exhibit nonlinear and nonplanar dynamics, similar to the behavior observed in the equivalent ground tests (Figs. 23, 25, and 27). As was observed in the uncoupled tests, it can also be concluded that the onset of the swirling motion is more gradual than observed in ground tests and that no sudden response jumps occur. In space, swirl also occurs over a wider frequency range. The softening frequency shift in the spacecraft and slosh modes is present in both the space and ground data.

Conclusions

The MODE ESM, when used on the ground and on the shuttle middeck, has demonstrated the ability to determine the dynamic characteristics of contained fluids for a wide range of tanks, fluid slosh natural frequencies, and gravity conditions. The space results demonstrated the ability of the hardware to resolve slosh forces to as low as 0.1 mN.

The existing linear models predicted the fluid slosh natural frequencies to within 5 to 35% and the damping ratios within 5%, but of course did not capture the nonlinear behavior, which becomes apparent for tank motions as little as 1% of the diameter. As a result, their application to microgravity fluid modeling is problematic.

When the results of all the MODE flat-bottom and spherical-bottom tank experiments are compared, the conclusion is that there is no significant difference in the dynamic slosh behavior. At lower fill levels the shape of the tank bottom would have an effect on the dynamic behavior.

In contrast with the nonlinear, nonplanar, and multiple-response slosh behavior observed in the silicone-oil ground experiments, the slosh behavior of this fluid is essentially linear in space. This is due to the very high damping ratio of the first slosh mode in space. However, in space both the uncoupled and the coupled water experiments exhibited nonlinear and nonplanar characteristics similar to those observed in the ground experiments. This is due to the relatively high restoring force for water, which originates from the contact-angle hysteresis.

The MODE space experimental results are being used to update and validate the MIT analytical model for microgravity conditions. The MODE results have established a database with which researchers can validate their analytical models. This may eventually lead to the reliable design and prediction tools that are necessary to meet the high performance requirements of future spacecraft.

Acknowledgments

This work was supported by the NASA OAST Instep Flight Experiments Program and the NASA Langley Research Center Reference NASI-18690, with Sherwin Beck as monitor; by the NASA Head Quarter Grant NAGW-1335 to the MIT Space Engineering Research Center, with Robert Hayduk as technical monitor, and by NASA Head Quarter Grant NAGW-2014 with Samuel Venneri as technical monitor.

References

[1]van Schoor, M. C., Peterson, L. D., and Crawley, E. F., "The Coupled Nonlinear Dynamic Characteristics of Contained Fluids in Zero Gravity," *Proceedings of the AIAA/ASME/ASCE/AHS 31st Structures, Structural Dynamics, and Materials Conference*, AIAA, Washington, DC, Pt. 4, pp. 2–43, 1990 (AIAA Paper 90-0966).

[2]Dodge, F. T., and Garza, L. R., "Experimental and Theoretical Studies of Liquid Sloshing at Simulated Low Gravity," *Transactions of the American Society of Mechanical Engineers, Journal of Applied Mechanics*, Vol. 34, Series E No. 3, 1967, pp. 555–561.

[3]Dodge, F. T., and Garza, L. R., "Simulated Low-Gravity Sloshing in Spherical Ellipsoidal and Cylindrical Tanks," *Journal of Spacecraft and Rockets*, Vol. 7, No. 3, 1970, pp. 204–206.

[4]Kuttler, J. R., and Sigillito, V. G., "Sloshing of Liquids in Cylindrical Tanks," *AIAA Journal*, Vol. 22, No. 2, 1984, pp. 309–311.

[5]Martin, R. E., "Effects of Transient Propellant Dynamics on Deployment of Large Liquid Stages in Zero-Gravity with Application to Shuttle/Centaur," International Astronautical Federation, IAF-86-119, 1986.

[6]Yeh, G. C. K., "Free and Forced Oscillations of a Liquid in a Axisymmetric Tank at Low-Gravity Environments," *Journal of Applied Mechanics*, Vol. 34, No. 1, 1967, pp. 23–28.

[7]Ganiev, R. F., "Nonlinear Resonance Oscillations of Bodies with a Liquid," *Soviet Applied Mechanics* (translated from *Prikladnaya Mekhanika*, Vol. 13, No. 10, 1977, pp. 23–29).

[8]Limarchenko, O. S., "Effect of Capillarity on the Dynamics of a Container-Liquid System," *Soviet Applied Mechanics* (translated from *Prikladnaya Mekhanika*, Vol. 17, No. 6, 1981, pp. 124–128).

[9]Limarchenko, O. S., "Application of a Variational Method to the Solution of Nonlinear Problems of the Dynamics of Combined Motions of a Tank with Fluid," *Soviet Applied Mechanics* (translated from *Prikladnaya Mekhanika*, Vol. 19, No. 11, 1983, pp. 100–104).

[10]Myshkis, A. D., Babskii, V. G., Kopachevskii, N. D., Slobozhanin, L. A., and Tyuptsov, L. A., *Low-Gravity Fluid Mechanics*, Springer–Verlag, New York, 1987.

[11]Crawley, E. F., van Schoor, M. C., and Bokhour, E. B., "The Middeck 0-Gravity Dynamics Experiment," NASA Contractor Report 4500, March 1993.

[12]Miles, J. W., "Internally Resonant Surface Waves in a Circular Cylinder," *Journal of Fluid Mechanics*, Vol. 149, 1984, pp. 1–14.

[13]Miles, J. W., "Resonantly Forced Surface Waves in a Circular Cylinder," *Journal of Fluid Mechanics*, Vol. 149, 1984, pp. 15–31.

[14]Luke, J. C., "A Variational Principle for a Fluid with a Free Surface," *Journal of Fluid Mechanics*, Vol. 27, No. 2, 1967, pp. 395–397.

[15]Abramson, H. N. (ed.), "The Dynamic Behavior of Liquids in Moving Containers," NASA SP-106, 1966.

[16]Satterlee, H. M., and Chin, J. H., "Meniscus Shape Under Reduced Gravity Conditions," 1965 in Cohan (1965).

[17]Reynolds, W. C., and Satterlee, H. M., "Liquid Propellant Behaviour at Low and 0-*g*," Ref. 15, pp. 387–439.

[18]Salzman, J. A., and Masica, W. J., "An Experimental Investigation of the Frequency and Viscous Damping of Liquids during Weightlessness," NASA TND-5058, 1969.

[19]Ross, H. R., and Pline, A. D., "Equilibrium Times for Gas-Liquid Systems Exposed to Step Changes in Gravity," American Inst. of Chemical Engineers Annual Meeting, Washington, DC, Dec. 1988.

[20]Weislogel, M. M., and Ross, H. D., "Surface Settling in Partially Filled Containers Upon Step Reduction in Gravity," NASA TM-103641, N91-14556, 1991.

[21]Case, M. M., and Parkinson, W. C., "Damping of Surface Waves in an Incompressible Fluid," *Journal of Fluid Mechanics*, Vol. 2, 1957, pp. 172–188.

[22]Cohan, H., and Rogers, M. (eds.), "Fluid Mechanics and Heat Transfer Under Low gravity," AD 633580, 1965.

E. A. Thornton
Associate Editor